



Original article

Onset of gyrotactic microorganisms in MHD Micropolar nanofluid flow with partial slip and double stratification

Iskander Tlili ^{a,b}, Muhammad Ramzan ^{c,d,*}, Habib Un Nisa ^c, Meshal Shutaywi ^e, Zahir Shah ^f, Poom Kumam ^{g,h,i,*}

^a Institute of Research and Development, Duy Tan University, Da Nang 550000, Vietnam

^b Faculty of Civil Engineering, Duy Tan University, Da Nang 550000, Vietnam

^c Department of Computer Science, Bahria University, 44000 Islamabad, Pakistan

^d Department of Mechanical Engineering, Sejong University, Seoul 143-747, South Korea

^e Department of Mathematics, College of Science & Arts, King Abdulaziz University, P. O. Box 344, Rabigh 21911, Saudi Arabia

^f Center of Excellence in Theoretical and Computational Science (TaCS-CoE), SCL 802 Fixed Point Laboratory, Science Laboratory Building, King Mongkut's University of Technology Thonburi (KMUTT), 126 Pracha-Uthit Road, Bang Mod, Thrung Khru, Bangkok 10140, Thailand

^g KMUTT Fixed Point Research Laboratory, Room SCL 802 Fixed Point Laboratory, Science Laboratory Building, Department of Mathematics, Faculty of Science, King Mongkut's University of Technology Thonburi (KMUTT), Bangkok 10140, Thailand

^h KMUTT-Fixed Point Theory and Applications Research Group, Theoretical and Computational Science Center (TaCS), Science Laboratory Building, Faculty of Science, King Mongkut's University of Technology Thonburi (KMUTT), Bangkok 10140, Thailand

ⁱ Department of Medical Research, China Medical University Hospital, China

ARTICLE INFO

Article history:

Received 13 November 2019

Revised 10 May 2020

Accepted 21 June 2020

Available online 30 June 2020

Keywords:

Bioconvective flow

Micropolar nanofluid

Nonlinear thermal radiation

Thermal and solutal stratification

Partial slip

ABSTRACT

The study of nanofluid dynamics under the influence of bioconvection has valuable applications as the nanofluids possess tremendous heat transfer capabilities in comparison to the ordinary fluids. Having such amazing characteristics of nanofluids in mind, the objective of the present study is to analyze the influence of bioconvective Micropolar nanofluid flow comprising gyrotactic microorganisms with the thermal and solutal stratifications at the boundary surface. The novelty of the present study is enhanced by adding the contribution of nonlinear thermal radiation with partial slip boundary condition. The Homotopy Analysis Method (HAM) is employed to address the highly nonlinear system of differential equations. This system of differential equations is an outcome of suitable transformations applied to the mathematical model described by the system of partial differential equations. Illustrations depicting influences of prominent parameters are supported by requisite discussions keeping in view their physical significance. It is comprehended that the local density number is deteriorated for Peclet and bioconvection Lewis numbers. It is also observed that fluid velocity is declined for growing estimates of bioconvection Rayleigh number.

© 2020 The Author(s). Published by Elsevier B.V. on behalf of King Saud University. This is an open access article under the CC BY-NC-ND license (<http://creativecommons.org/licenses/by-nc-nd/4.0/>).

* Corresponding authors at: Department of Computer Science, Bahria University, 44000 Islamabad, Pakistan (M. Ramzan), KMUTT Fixed Point Research Laboratory, Room SCL 802 Fixed Point Laboratory, Science Laboratory Building, Department of Mathematics, Faculty of Science, King Mongkut's University of Technology Thonburi (KMUTT), Bangkok 10140, Thailand (P. Kumam).

E-mail addresses: mramzan@bahria.edu.pk (M. Ramzan), poom.kum@kmutt.ac.th (P. Kumam).

Peer review under responsibility of King Saud University.



Production and hosting by Elsevier

1. Introduction

The swimming trait of gyrotactic microorganisms is vital to comprehend numerous ecological facts related to bioconvection. It was Platt who floated the idea of "Bioconvection" *i.e.*, dispersion of gyrotactic microorganisms in shallow suspensions. Bioconvection is the macroscopic convective motion of fluid caused by the density gradient and is created by the collective swimming of motile microorganisms. The development of bioconvection enhances mixing and slows down the settling of particles. Unlike natural convection, bioconvection is caused by unstable density stratification. Because of this, variation in density due to the movement of motile microorganisms is suggested to the momentum governing equation (Kuznetsov and Avramenko, 2004; Makinde

and Animasaun, 2016; Makinde and Animasaun, 2016). Kuznetsov (Kuznetsov, 2010) studied the characteristics of bioconvection comprising gyrotactic microorganisms immersed in a nanofluid flow using the Galerkin method. It is concluded in this exploration that the inclusion of gyrotactic microorganisms always destabilizes the nanofluid flow containing nanoparticles in comparison to the nanofluid flow in the absence of gyrotactic microorganisms. Nayak et al. (Nayak et al., 2020) numerically analyzed the flow of 3D bioconvective Casson nanofluid with motile organisms and multiple slips. The additional effects taken into account are thermal and solutal stratifications and chemical species. The major outcome of this exploration is that large estimates of Peclet number result in a decline in the local Sherwood number. The water-based nanofluid flow comprising single and multi-walled carbon nanotubes amalgamated with motile microorganisms over a vertical cone is studied by Ramzan et al. (2019a–c). The conclusion of the model reveals the velocity field is diminished for increasing estimates of buoyancy ratio parameter and bioconvection Rayleigh number. Recently, Waqas et al. (Waqas et al., 2020) extracted the numerical solution of the Carreau–Yasuda nanofluid flow in the presence of gyrotactic microorganisms and second-order slip using `bvp4c` MATLAB function. The key observation of this research is that the density of motile microorganisms is deteriorated for growing values of Peclet number and bioconvection Lewis number. The flow of magnetized nanofluid owing to a paraboloid revolution under the influence of gyrotactic microorganisms is studied by Khan et al. (2020a,b). Some more studies highlighting gyrotactic microorganisms may be found at (Kumar et al., 2019; Alshomrani and Ramzan, 2019; Ramzan et al., 2017a–d; Khan et al., 2020a,b; Shahid et al., 2018) and many therein.

Over the past few years, the requirement to model and shape the fluid that comprises rotating micro-constituents have given rise to the Micropolar fluid theory. The fluids that couple the particle rotatory motion and macroscopic velocity field are known as Micropolar fluids. Such fluids are made of stiff elements that are cuddled in a sticky or viscous conduit. Examples of such fluids are blood flow, bubbly liquid, and Ferrofluids. The industrial applications of these fluids are biological structures, lubricant fluids, and polymer solutions. The notion of Micropolar fluid model is originally floated by Eringen (Eringen, 1966). Later, numerous investigations are conducted focusing on this important non-Newtonian fluid. The flow of Micropolar fluid influenced by a strong magnetic field past a heated/cooled extended spongy surface with mixed convection is studied by Turkyilmazoglu (Turkyilmazoglu, 2017). The exact analytical solution of the proposed model is obtained using Mathematica software. The outcome of the model divulges that the heat transfer rate is decreased for the positive values of the material parameter, however, an opposite trend is witnessed for negative estimates. Ahmad et al. (Ahmad et al., 2020) studied the Micropolar nanofluid flow with Cattaneo–Christov heat flux, entropy generation analysis, and slip condition at the boundary of a stretched surface. The solution of the envisioned mathematical model is obtained numerically. One of the salient results of the discussion is that the magnetic effect strengthened the microrotation. The Micropolar nanofluid flow in a permeable chamber with thermal radiation and thermo-gravitational transmission under the effect of a uniform magnetic field is studied by Izadi et al. (Izadi et al., 2020). Nadeem et al. (Nadeem et al., 2020) analyzed heat transfer analysis in the 3D flow of Micropolar fluid through an exponentially extended surface. The key observation of this study is that the temperature and concentration of the fluid are improved for the Micropolar parameter. Some other related work on Micropolar fluid can be found in (Ramzan et al., 2016; Ramzan et al., 2017a–d; Koriko et al., 2019; Ramadevi et al., 2020).

Heat transfer in nanofluid flows has drawn substantial attention during the last two decades. Nanofluid is a liquid that is made by the insertion of metallic particles with dimensions (<100 nm) in a conventional fluid like water, engine oil, and ethylene glycol. These conventional fluids have restricted heat transfer abilities and are therefore unable to encounter today industrial cooling necessities. Suspended nanoparticles in any base fluid can improve the fluid heat transfer features. Researchers and scientists have revealed interesting aspects of nanofluids. Gireesha et al. (Gireesha et al., 2018) analyzed the dusty flow of a nanofluid with Hall current effect over an extended surface. The numerical solution of the proposed model is analyzed via the RK Fehlberg integration scheme. It is disclosed in this study that Hall current and time-dependency are major ingredients for the enhancement of heat transfer rate. The time-dependent nanofluid flow comprising engine oil as base fluid and TiO_2 as nanoparticles with Hall current effects, nonlinear thermal radiation, and exponential heat source over an isothermal planar surface are examined by Mahanthesh et al. (Mahanthesh et al., 2019). This study revealed that nanofluid temperature is enhanced when the solid volume fraction of nanoparticles is strengthened. Sheikholeslami (Sheikholeslami, 2019) used a new numerical scheme named Control Volume Based Finite Element Method (CVFEM) to examine the nanofluid flow under the influence of strong Lorentz force in a permeable media with exergy and entropy analysis. It is discussed in this exploration that exergy loss enhances when a strong magnetic field is applied. The flow of MHD hybrid nanofluid comprising MoS_2 –Ag and $\text{C}_2\text{H}_6\text{O}_2$ – H_2O is studied numerically in the presence of Joule heating over an isothermal wedge by Mahanthesh et al. (Mahanthesh et al., 2020). It is determined in this research that the viscosity of the fluid is enhanced when the magnetic force is bolstered. Lu et al. (2018a,b) discussed the Micropolar nanofluid passed a linear stretched surface under the effect of homogenous and heterogeneous reactions. A marvelous recent work in this regard is done by Wakif et al. (Wakif et al., 2019) who designed a meta survey of thermophoresis impact in various scenarios by discussing sixty published papers. A similar work discussing the impact of Brownian motion in the form of *meta*-analysis is performed by Animasaun et al. (2019). Some interesting features of nanofluid can also be seen in references (Gireesha et al., 2018; Hajizadeh et al., 2020; Kumar et al., 2018; Tlili et al., 2020; Mahanthesh et al., 2019; Alebraheem and Ramzan, 2019; Turkyilmazoglu, 2019; Turkyilmazoglu, 2018; Ahmad et al., 2017; Nayak et al., 2019; Akbar et al., 2018; Nayak et al., 2017; Nayak et al., 2017; Turkyilmazoglu, 2019).

The key function of the thermal radiation is to control the transfer of heat. By monitoring heat aspects to a particular range, one can improve the quality of the refined product. In the transfer of heat flow, the influence of thermal radiation is extremely significant for a system operating at an above-average temperature where radiation from heated walls and working fluid is different. Sheikholeslami et al. (2019) explored the flow of Electrohydrodynamic nanofluid in a wavy permeable chamber with thermal radiation numerically. The Control Volume Based Finite Element Method (CVFEM) is employed to handle the highly nonlinear system. The major outcome of the presented study is that the thermal transmission and convective circulation are improved for large values of permeability of the porous media. The impact of gyrotactic microorganisms in a thermal radiative nanofluid flow with both types of carbon nanotubes over a vertical cone in a spongy media is explored by Ramzan et al. (2019). Turkyilmazoglu (2019) analyzed the effect of thermal radiation on heat transfer flow past a vertical extended sheet with free convection and temperature-dependent heat generation/absorption in a porous media. Exact closed-form solutions for the said problem

are found. It is concluded that the heat transfer rate is enhanced in the case of the sink and the opposite behavior is monitored for source. The time-dependent rotational flow of nanofluid comprising dust particles and carbon nanotubes past a vertical extended surface with thermal radiation and Hall current in a Darcy-Forchheimer permeable medium is studied by Bilal and Ramzan. (Bilal and Ramzan, 2019). The problem is solved numerically using MATLAB software. Some recent investigations highlighting the thermal radiation effect are given at (Turkyilmazoglu, 2016; Ramzan et al., 2017a–d; Li et al., 2019; Sheikholeslami et al., 2018; Suleman et al., 2018; Lu et al., 2018a,b) and many therein.

The role of stratification in heat and mass transfer is essential. In nanofluids, stratification occurs in layer formations due to variation in both heat and mass profiles. That is why the simultaneous occurrence of both distributions is the key factor for thermal and solutal stratifications. Industrial foods, subterranean water storage, and the presence of heterogeneous amalgams in the atmosphere are a few examples of stratification. The function of stratification in lakes is vital as it maintains a balance between the oxygen and hydrogen ratio by regulating the difference between temperature and concentration and keeping the environment favorable for the evolution of species. Moreover, the role of thermal stratification is vital in solar engineering as it is the main ingredient to boost the efficiency of the system. Studies highlighting the different aspects of stratification may be quoted in this regard. Waqas et al. (2020) studied the flow of thixotropic nanofluid flow in a stratified medium with nonlinear convection past a convectively heated extended surface. It is analyzed that both stratified fields are enhanced when values of Biot number is increased. The viscous nanofluid flow with thermal stratification past a moving thin needle is analyzed by Ramzan et al. (2020). The key observation of this study divulged that fluid temperature diminishes for large estimates of the thermal stratification parameter. Ahmad et al. (2020) deliberated the nanofluid flow with both types of carbon nanotubes past a static wedge with double stratification. It is observed in this exploration that both thermal and concentration profiles are decreased for thermal and solutal stratifications respectively. Some more recent explorations featuring stratification are given at (Daniel et al., 2020; Khan et al., 2017; Naz et al., 2020; Ramzan et al., 2016, 2019; Rosseland, 2013; Ramzan et al., 2019c).

From the above literature review, it is revealed that less attention is paid towards the consequence of gyrotactic microorganisms on Micropolar nanofluid flow. However, no work is done so far on bioconvective MHD flow of Micropolar nanofluid in attendance of nonlinear thermal radiation in a thermal and solutal stratified medium with partial slip. The present analysis aims to fill this gap and scrutinized the influence of nonlinear thermal radiation on bioconvective MHD flow of Micropolar nanofluid with partial slip and double stratification at the boundary. The analytical solution of transformed governing equations is attained via the Homotopy Analysis Method. The results are displayed graphically and discussed accordingly.

The present study facilitates the existing literature to answer the following critical questions:

- i. How bioconvection Rayleigh number affect the velocity and the Motile density fields?
- ii. What are the effects of the Brownian motion and thermophoresis parameters on the fluid's temperature?
- iii. Why fluid velocity is diminished due to growing estimates of suction parameter?
- iv. How local density number behave for Peclet and bioconvection Lewis numbers?
- v. What are the impacts of thermal and solutal stratifications on the respective heat and mass transfer phenomena?

2. Mathematical Formulation:

Consider a two-dimensional, MHD Micropolar incompressible nanofluid flow along a preamble stretched surface having slip condition at the boundary. The behavior of flow is under the influence of the uniform electric and magnetic field. The induced magnetic field effects are ignored owing to small Reynolds number. The non-Newtonian nanofluid flow is under the impact of the Bioconvective boundary layer with gyrotactic microorganisms and thermal and solutal stratifications (Fig. 1).

Using the approximations of the boundary layer, governing equations representing the envisioned model are as follows (Ramzan et al., 2017a–d; Naz et al., 2020):

$$\frac{\partial u}{\partial x} + \frac{\partial v}{\partial y} = 0, \tag{1}$$

$$u \frac{\partial u}{\partial x} + v \frac{\partial u}{\partial y} = \left(\frac{\mu + k}{\rho_f} \right) \frac{\partial^2 u}{\partial y^2} + \frac{k}{\rho_f} \frac{\partial N}{\partial y} + \frac{\sigma}{\rho_f} (E_0 B_0 - B_0^2 u) + \frac{1}{\rho_f} [(\beta^* - C_\infty \beta^*)g(T - T_\infty)\rho_f - (\rho_p - \rho_f)g(C - C_\infty) - \gamma(n - n_\infty)g(\rho_m - \rho_f)], \tag{2}$$

$$u \frac{\partial N}{\partial x} + v \frac{\partial N}{\partial y} = \frac{\gamma^*}{\rho_j} \frac{\partial^2 N}{\partial y^2} - \frac{k}{\rho_j} \left(2N + \frac{\partial u}{\partial y} \right), \tag{3}$$

$$u \frac{\partial T}{\partial x} + v \frac{\partial T}{\partial y} = \alpha_1 \frac{\partial^2 T}{\partial y^2} + \tau D_B \frac{\partial T}{\partial y} \frac{\partial C}{\partial y} + \tau \frac{D_T}{T_\infty} \left(\frac{\partial T}{\partial y} \right)^2 - \frac{1}{(\rho c)_f} \frac{\partial q_r}{\partial y}, \tag{4}$$

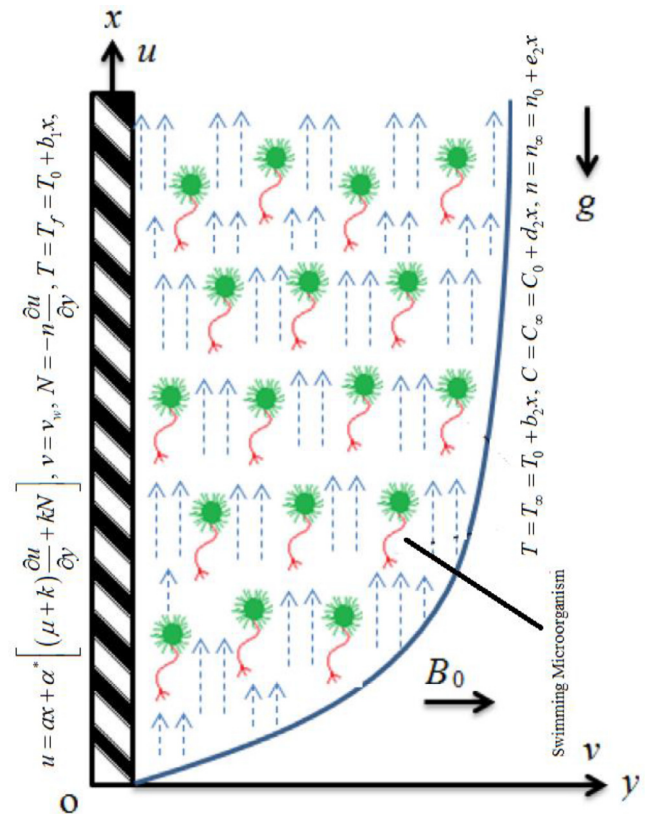


Fig. 1. Illustration of the flow pattern.

$$u \frac{\partial C}{\partial x} + v \frac{\partial C}{\partial y} = \left[D_B \left(\frac{\partial^2 C}{\partial y^2} \right) + \frac{D_T}{T_\infty} \left(\frac{\partial^2 T}{\partial y^2} \right) \right], \tag{5}$$

$$u \frac{\partial n}{\partial x} + v \frac{\partial n}{\partial y} + \frac{bW_c}{(C_f - C_\infty)} \left[\frac{\partial}{\partial y} \left(n \frac{\partial C}{\partial y} \right) \right] = D_m \left(\frac{\partial^2 n}{\partial y^2} \right). \tag{6}$$

With boundary conditions:

$$\begin{aligned} u &= ax + \alpha * \left[(\mu + k) \frac{\partial u}{\partial y} + kN \right], \quad v = v_w, \quad N = -n \frac{\partial u}{\partial y}, \quad T = T_f = T_0 + b_1 x, \\ C &= C_f = C_0 + d_1 x, \quad n = n_f = n_0 + e_1 x \text{ at } y = 0 \\ T &= T_\infty = T_0 + b_2 x, \quad C = C_\infty = C_0 + d_2 x, \quad n = n_\infty = n_0 + e_2 x \\ u &\rightarrow 0, \quad N \rightarrow 0, \text{ as } y \rightarrow \infty. \end{aligned} \tag{7}$$

Here, (u, v) , $\mu, k, \rho_f, E_0, B_0, \beta^*, \gamma^*, j, C, C_\infty, T, T_\infty$, and g represent velocity components in x - and y -directions, dynamic viscosity, vortex viscosity, nanofluid density, applied electric field, applied magnetic field strength, coefficient of volumetric volume expansion of Micropolar nanofluid, spin gradient viscosity, micro-rotation or angular velocity, the concentration of nanoparticles, free stream concentration of nanoparticles, temperature of the fluid, ambient temperature and gravity respectively. Furthermore, $(b_1, d_1, e_1, b_2, d_2, e_2) \rho_m, N, \tau, D_B, D_T, (\rho C)_f, q_r, Wc, T_f, T_0, C_f, C_0, n_f, n_0$, and n_∞, D_m , depict the constants, density of motile microorganisms, angular velocity, the ratio of effective heat capacity of nanoparticles to the base fluid, Brownian diffusion coefficient, thermophoresis diffusion coefficient, heat capacity of the fluid, radiative heat flux, maximum cell swimming speed, Convective fluid temperature, fluid reference temperature, Convective fluid concentration, reference concentration of nanoparticles, Convective fluid microorganism, reference concentration of microorganism, and ambient concentration of microorganisms, microorganism diffusion coefficient respectively. Eq. (6) represents the boundary layer equation for bioconvective flow. The radiative heat flux q_r considering Rosseland assumption (Rosseland, 2013) is given by:

$$q_r = - \frac{4\sigma^*}{3k^*} \frac{\partial T^4}{\partial y}, \tag{8}$$

Here, σ^* and k^* are the Stefan-Boltzmann constant and the mean absorption coefficient respectively. Assuming the temperature difference flow takes the form in such a way that T^4 is expanded about T_∞ in Taylor's series form. i.e.,

$$T^4 \approx 4T_\infty^3 T - 3T_\infty^4. \tag{9}$$

Invoking Eq. (9) into Eq. (8), we obtain

$$q_r = - \frac{16\sigma^* T_\infty^3}{3k^*} \frac{\partial T}{\partial y} \tag{10}$$

Now, plugging in values of q_r from Eq. (10) into the Eq. (4), we obtain

$$u \frac{\partial T}{\partial x} + v \frac{\partial T}{\partial y} = \alpha_1 \frac{\partial^2 T}{\partial y^2} + \tau D_B \frac{\partial T}{\partial y} \frac{\partial C}{\partial y} + \tau \frac{D_T}{T_\infty} \left(\frac{\partial T}{\partial y} \right)^2 + \frac{16}{(\rho C)_f} \sigma^* \frac{T_\infty^3}{3k^*} \frac{\partial^2 T}{\partial y^2}. \tag{11}$$

Dimensionless form of the above mathematical model is obtained by utilizing the following transformations:

$$\begin{aligned} \eta &= \sqrt{\frac{3U}{4\nu x}} y, \quad \psi = \sqrt{\frac{4\nu x U}{3}} f(\eta), \quad N = U \sqrt{\frac{3U}{4\nu x}} g(\eta), \\ \phi(\eta) &= \frac{C - C_\infty}{C_f - C_\infty}, \quad \xi(\eta) = \frac{n - n_\infty}{n_f - n_\infty}, \quad \theta = \frac{T - T_\infty}{T_f - T_\infty}, \quad U = \sqrt{2ax}, \end{aligned} \tag{12}$$

with U is the free stream velocity (Khan et al., 2017) and

$$T = T_\infty [1 + (\theta_w - 1)\theta], \tag{13}$$

where

$$\theta_w = \frac{T_f}{T_\infty}, \tag{14}$$

with θ_w is the temperature ratio parameter, Here, the satisfaction of equation (1) is inevitable. However, Eqs. (2), (3), (5), (6), (11), and (12) take the form:

$$\begin{aligned} (1 + K)f'''' + \frac{2}{3}(ff'' - f'^2) + Kg' - \frac{2}{3}Haf' + \frac{2}{3}HaE \\ + (\beta\theta - \omega\phi - Rb\xi) = 0, \end{aligned} \tag{15}$$

$$\left(1 + \frac{K}{2} \right) g'' + fg' - f'g - K(2g + f'') = 0, \tag{16}$$

$$\begin{aligned} \left[1 + \frac{4}{3} Rd \{ 1 + (\theta_w - 1)\theta \}^3 \right] \theta'' \\ + 4Rd [(\theta_w - 1)\{ 1 + (\theta_w - 1)\theta \}^2] \theta'^2 \\ + Pr \left[\theta' \phi' Nb + \theta'^2 Nt + \frac{2}{3} f \theta' - \frac{2}{3} f'(S + \theta) \right] = 0, \end{aligned} \tag{17}$$

$$\phi'' + Le(f\phi' - f'\phi) - LePf' + \frac{Nt}{Nb} \theta'' = 0, \tag{18}$$

$$\xi'' + Lb(f\xi' - f'\xi) - LbQf' - Pe[\phi''(\xi + \Omega) + \phi'\xi'] = 0. \tag{19}$$

with

$$\begin{aligned} f = f_w, \quad f' = 1 + \alpha(1 + K)f'', \quad g = nf'', \quad \theta = 1 - S, \\ \phi = 1 - P, \quad n = 1 - Q, \text{ at } \eta = 0 \\ f' = 0, \quad g = 0, \quad \theta = 0, \quad \phi = 0, \quad n = 0, \text{ at } \eta = \infty. \end{aligned} \tag{20}$$

The parameters in dimensionless form mention above $Lb, Le, Pe, \Omega, Pr, E, S, \alpha, Nt, Nb, P, Q, \beta, \omega$,

Rb, K, Ha, Rd , and f_w are Bioconvective Lewis number, Lewis number, Bioconvection Peclet number, Microorganisms concentration difference parameter, Prandtl number, Electric parameter, thermal stratification parameter, slip parameter, Thermophoresis parameter, Brownian motion parameter, Concentration stratification parameter, Motile density stratification parameter, buoyancy parameter depending on volumetric expansion coefficient of Micropolar nanofluid due to temperature, Buoyancy ratio, Bioconvection Rayleigh number, Material parameter, Hartmann number, Radiation parameter, and Suction parameter respectively. The values of these distinct dimensionless parameters arising in the above equations are characterized as:

$$\begin{aligned} Lb = \frac{\nu}{D_m}, \quad Le = \frac{\nu}{D_B}, \quad Pe = \frac{bW_c}{D_m}, \quad \Omega = \frac{n_\infty}{n_f - n_\infty}, \quad Pr = \frac{\nu}{\alpha_1}, \quad E = \frac{E_0}{u_w B_0}, \\ S = \frac{b_2}{d_1}, \quad \alpha = \alpha * \mu \sqrt{\frac{a}{\nu}}, \quad Nt = \frac{\tau D_T (T_f - T_\infty)}{\nu T_\infty}, \quad Nb = \frac{\tau D_B (C_f - C_\infty)}{\nu}, \\ P = \frac{d_2}{d_1}, \quad Q = \frac{e_2}{e_1}, \quad \omega = \frac{(\rho_p - \rho_f)(C_f - C_\infty)}{(1 - C_\infty)(T_f - T_\infty)\rho_f \beta^*}, \quad \beta = \frac{2\beta^*(1 - C_\infty)g(T_f - T_\infty)}{3a\rho_f}, \\ Rb = \frac{\gamma(\rho_m - \rho_f)(n_f - n_\infty)}{(1 - C_\infty)(T_f - T_\infty)\rho_f \beta^*}, \quad K = \frac{k}{\mu}, \quad Ha = \frac{\sigma B_0^2}{\rho a}, \quad Rd = \frac{4\sigma^* T_\infty^3}{k_1 k^*}, \quad f_w = -(av)^{-\frac{1}{2}} v_w. \end{aligned} \tag{21}$$

Local Sherwood number, Skin friction coefficient, the local density of motile microorganisms and local Nusselt of the motile microorganisms are given by:

Table 1

Series solution convergence for the assorted order of estimates when $Nt = 0.2, \alpha = 0.5, Rd = 0.6, \delta = 0.4, Pr = 1.6, Lb = 1.0,$ and $Ha = E = 0.7, \theta_w = 1.01, \beta = 0.1, \omega = 0.1,$ and $Rb = 0.1$

Order of approximation	$-f''(0)$	$-g''(0)$	$-\theta'(0)$	$-\phi'(0)$	$-\xi'(0)$
1	0.44635	0.08543	0.22612	0.56251	0.90410
5	0.45601	0.08784	0.23234	0.56718	0.91824
10	0.46343	0.09877	0.31419	0.56843	0.92260
15	0.47901	0.09882	0.36242	0.57309	0.93545
20	0.47919	0.09910	0.38927	0.57724	0.93909
25	0.47924	0.09987	0.39210	0.58054	0.94410
30	0.47924	0.09987	0.39210	0.58054	0.94410

$$Sh_x = \frac{xq_m}{D_B(C_f - C_\infty)}, Cf_x = \frac{2\tau_w}{\rho(ax)^2}, Nn_x = \frac{xq_n}{D_n(n_f - n_\infty)},$$

$$Nu_x = \frac{xq_w}{k_2(T_f - T_\infty)} \tag{22}$$

where

$$q_m = -D_B \left(\frac{\partial \phi}{\partial y} \right)_{y=0}, \tau_w = \left((\mu + k) \frac{\partial u}{\partial y} + kN \right)_{y=0}, q_n = -D_n \left(\frac{\partial \zeta}{\partial y} \right)_{y=0},$$

$$q_w = -k_1 \left(1 + \frac{16\sigma^* T_\infty^3}{k_1 k^*} \right) \left(\frac{\partial T}{\partial y} \right)_{y=0}. \tag{23}$$

Dimensionless forms of Skin friction coefficient, Nusselt & Sherwood numbers, and motile microorganism density are appended as follows:

$$Sh_x Re_x^{-1/2} = -\phi'(0), \frac{1}{2} Cf_x Re_x^{1/2} = [1 + (1 - n)K] f''(0), Nn_x Re_x^{-1/2} = -\zeta'(0),$$

$$Nu_x Re_x^{-1/2} = - \left[1 + \frac{4}{3} Rd \{ (\theta_w - 1) \theta(0) \}^3 \right] \theta'(0), \tag{24}$$

with $Re_x = \frac{u_0 x^2}{\nu}$ is the local Reynolds number.

3. HAM solution:

The acceptable preliminary approximations and corresponding linear operators are defined as:

$$f_0(\eta) = f_w + \frac{1}{1+\alpha(1+K)} (1 - e^{-\eta}), \quad g_0(\eta) = \frac{n}{1+\alpha(1+K)} e^{-\eta},$$

$$\theta_0(\eta) = (1 - S)e^{-\eta}, \tag{25}$$

$$\phi_0(\eta) = (1 - P)e^{-\eta}, \quad \zeta_0(\eta) = (1 - Q)e^{-\eta}.$$

$$L_f = f''' - f', \quad L_g = g'' - g, \quad L_\theta = \theta'' - \theta,$$

$$L_\phi = \phi'' - \phi, \quad L_\zeta = \zeta'' - \zeta. \tag{26}$$

The above-mentioned linear operators obey the below-mentioned properties:

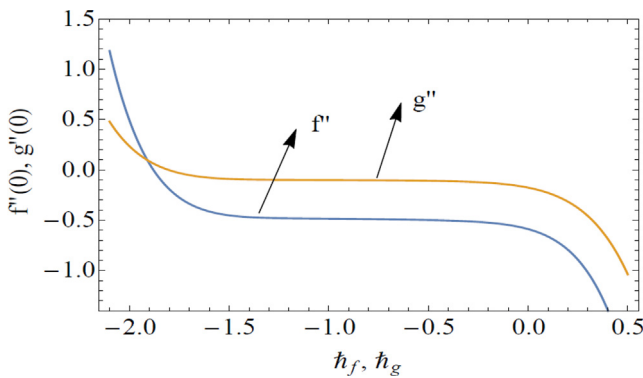


Fig. 2a. *h*-curves for *f, g*.

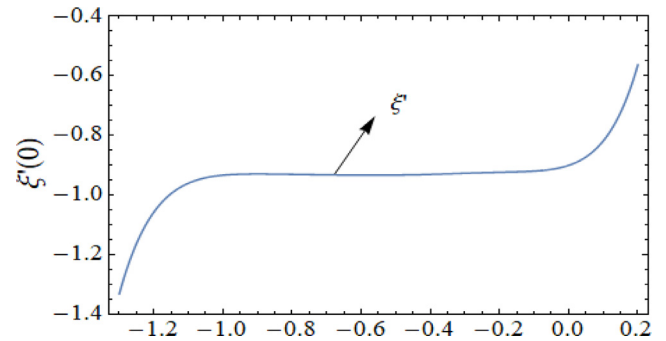


Fig. 2c. *h*-curves for ξ .

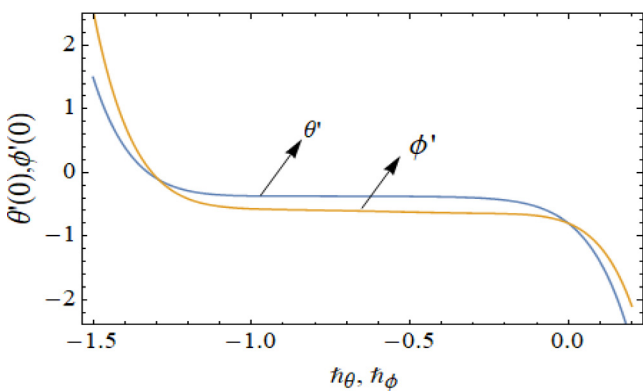


Fig. 2b. *h*-curves for θ, ϕ .

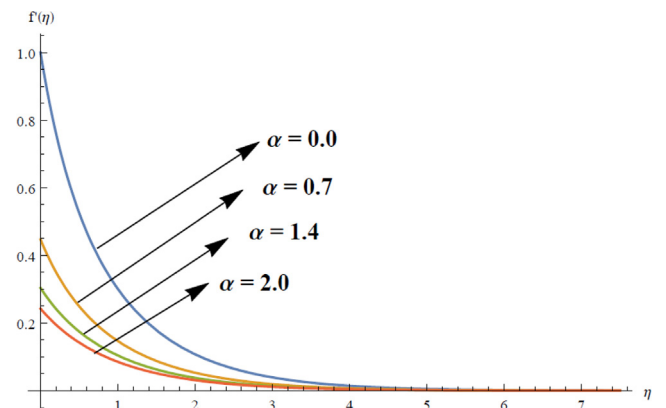


Fig. 3. Response of $f'(\eta)$ versus varied estimates of $\alpha = 0.0, 0.7, 1.4, 2.0$.

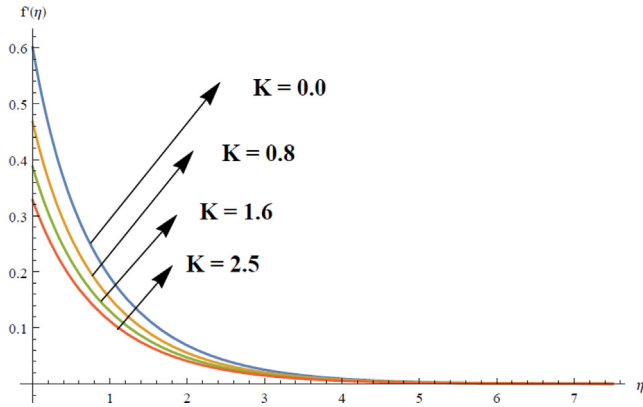


Fig. 4. Response of $f'(\eta)$ versus varied estimates of $K = 0.0, 0.8, 1.6, 2.5$.

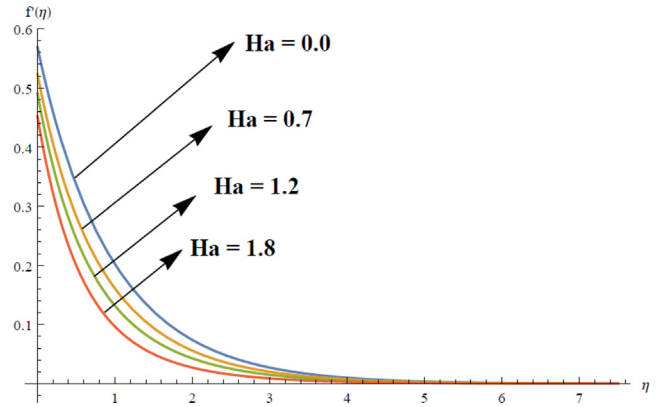


Fig. 6. Response of $f'(\eta)$ versus varied estimates of $Ha = 0.0, 0.7, 1.2, 1.8$.

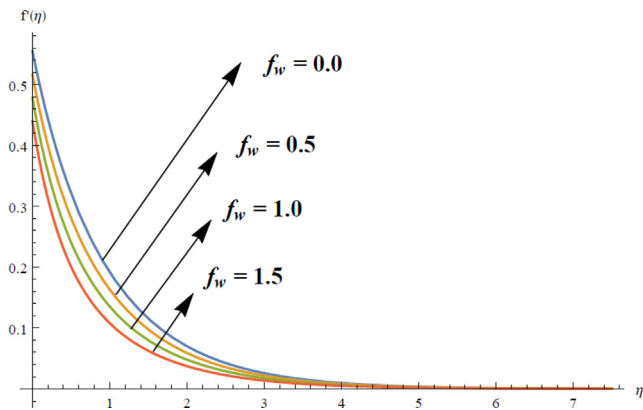


Fig. 5. Response of $f'(\eta)$ versus varied estimates of $f_w = 0.0, 0.5, 1.0, 1.5$.

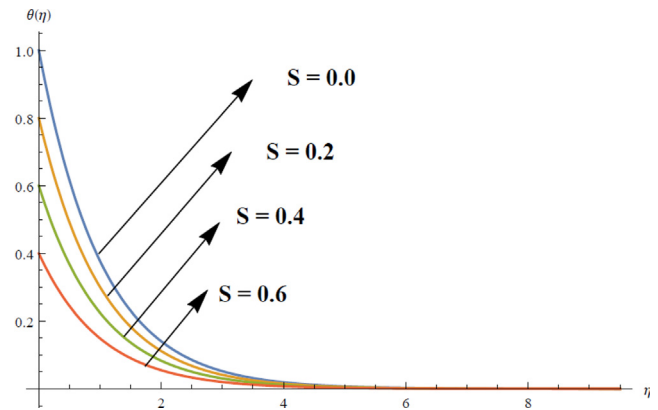


Fig. 7. Response of $\theta(\eta)$ versus varied estimates of $S = 0.0, 0.2, 0.4, 0.6$.

$$L_f\{H_1 + H_2e^{-\eta} + H_3e^{\eta}\} = 0, L_g\{H_4e^{-\eta} + H_5e^{\eta}\} = 0, L_\theta\{H_6e^{-\eta} + H_7e^{\eta}\} = 0, L_\phi\{H_8e^{-\eta} + H_9e^{\eta}\} = 0, L_\zeta\{H_{10}e^{-\eta} + H_{11}e^{\eta}\} = 0. \tag{27}$$

where $H_i = (i = 1$ to $11)$, represent the arbitrary constants.

4. Convergence analysis

The Homotopy Analysis technique is utilized to find the analytical solution and is subject to the auxiliary parameters $h_f, h_g, h_\theta, h_\phi$ and h_ζ . These parameters are essential to control and normalize the convergence zone of series solutions. The admissible ranges of these parameters are $-1.4 \leq h_f \leq -0.3, -1.4 \leq h_g \leq -0.3, -1.1 \leq h_\theta \leq -0.25, -1.2 \leq h_\phi \leq -0.25$ and $-0.9 \leq h_\zeta \leq -0.2$. The values obtained in Table 1 are in total consensus to the curves shown in Figs. 2(a)–2(c). An excellent concurrence between the graphical and numerical outcomes is seen. Table 1 expresses the series solutions' convergence for momentum, energy equation, concentration, and bioconvection and demonstrates that the 25th order of guesses is adequate for the convergent series solution that is in good agreement to the graphical illustration shown in Figs. 2(a)–2(c).

5. Results and discussion

This section is earmarked to analyze the impacts of numerous parameters on associated profiles. The values of the involved parameters are fixed as $Nt = 0.2, \alpha = 0.5, Rd = 0.6, \delta = 0.4, Pr = 1.6,$

$Lb = 1.0, Ha = E = 0.7, \theta_w = 1.01, \beta = 0.1, \omega = 0.1, Rb = 0.1,$ unless stated. Fig. 3 is drawn to witness the relationship between the slip parameter α and the velocity of the fluid. It is seen that velocity in on decline for higher estimates of α . The slip boundary condition at the wall is employed when the viscosity effect of the fluid at the wall is negligible. More resistance is encountered in transferring the stretching velocity to the fluid flow owing to the weak bond between fluid and the wall as of the partial slip. Thus, velocity diminishes for large estimates of slip parameter. Fig. 4 portrays the connection between the material parameter K and the velocity profile. It is noticed that velocity distribution is decreasing function

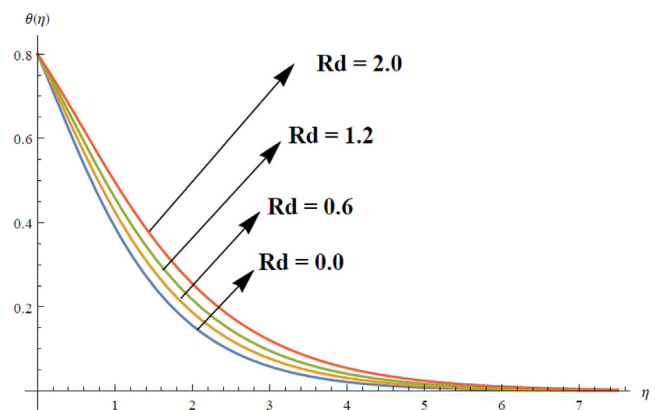


Fig. 8. Response of $\theta(\eta)$ versus varied estimates of $Rd = 0.0, 0.6, 1.2, 2.0$.

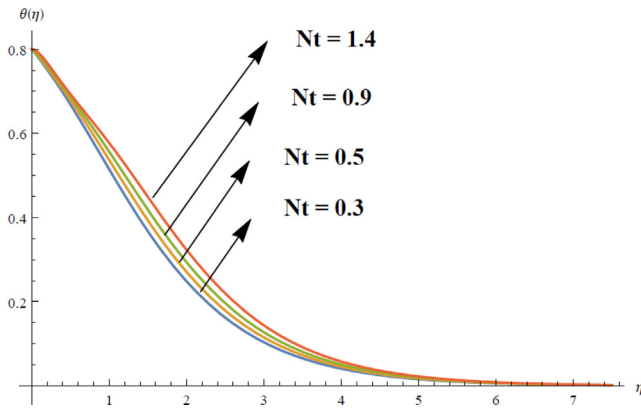


Fig. 9. Response of $\theta(\eta)$ versus varied estimates of $Nt = 0.3, 0.5, 0.9, 1.4$.

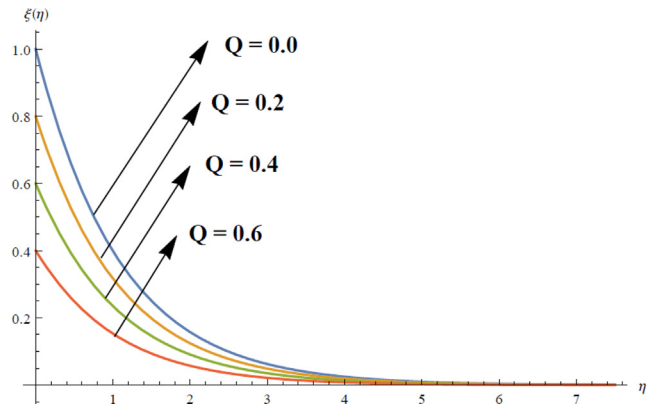


Fig. 12. Response of $\xi(\eta)$ versus varied estimates of $Q = 0.0, 0.2, 0.4, 0.6$.

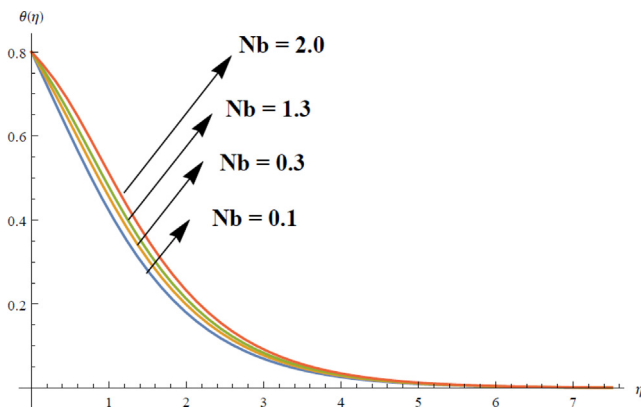


Fig. 10. Response of $\theta(\eta)$ versus varied estimates of $Nb = 0.1, 0.3, 1.3, 2.0$.

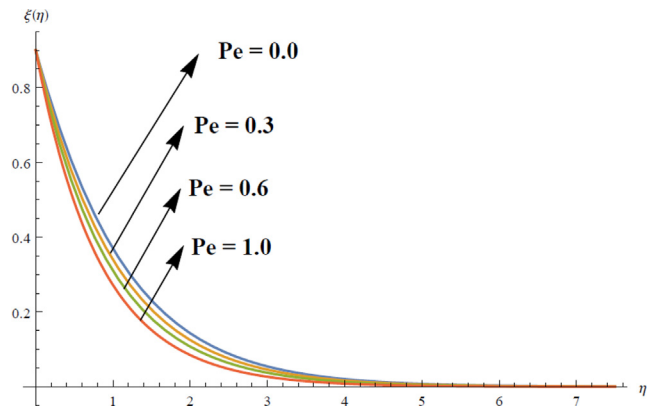


Fig. 13. Response of $\xi(\eta)$ versus varied estimates of $Pe = 0.0, 0.3, 0.6, 1.0$.

of K . The material parameters allow altering the design of the material without having to restructuring the material. It can be comprehended from the figure that the velocity of the fluid is high in the vicinity of the wall and diminishes as it moves away from it due to increased estimates of K . The impression of the suction parameter f_w on the velocity profile is portrayed in Fig. 5. It is comprehended that velocity is a diminishing function of f_w . The suction is the process of sucking owing to the formation of a vacuum in a cavity or a surface. In fact, velocity is weaker versus large estimates of f_w . Furthermore, the velocity boundary layer becomes thinner near the wall due to increment in the suction parameter.

Fig. 6 illustrates the association of the Hartmann number Ha with the velocity field. Velocity is weakened owing to large estimates of Ha . The Hartmann number is the quotient of the electromagnetic force and the viscous force. Stronger Lorentz force hinders the movement of the fluid motion and consequences in the form of weaker velocity. The relationship between the thermal stratification parameter S and the temperature is depicted in Fig. 7. Thermal stratification is the creation of two discrete layers of water in a lake at different temperatures. Higher values of S produce more temperature differences between the surfaces and ultimately reduce the

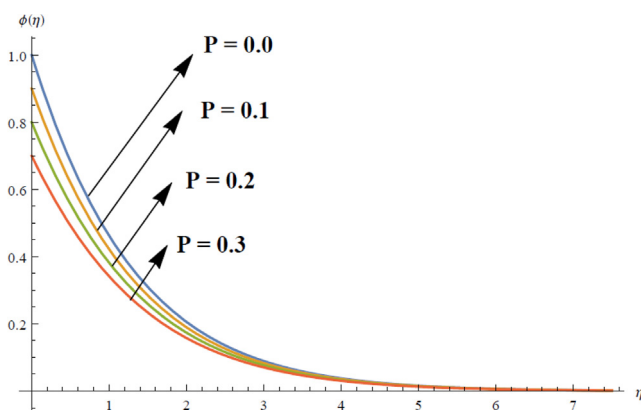


Fig. 11. Response of $\phi(\eta)$ versus varied estimates of $P = 0.0, 0.1, 0.2, 0.3$.

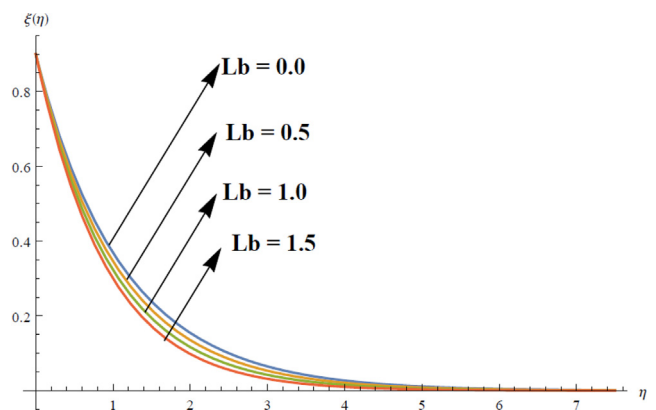


Fig. 14. Response of $\xi(\eta)$ versus varied estimates of $Lb = 0.0, 0.5, 1.0, 1.5$.

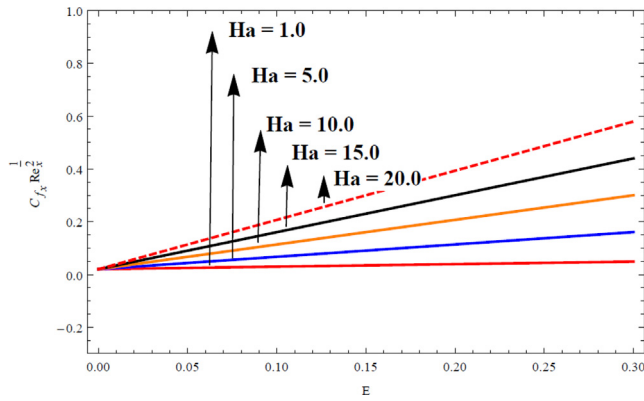


Fig. 15. Effect of $Cf_x Re_x^{-1/2}$ versus varied estimates of E and Ha .

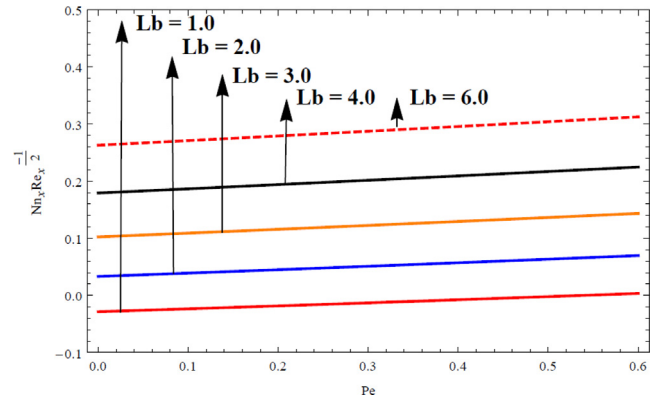


Fig. 18. Effect of $Nn_x Re_x^{-1/2}$ versus varied estimates of Pe and Lb .

temperature of the fluid. Fig. 8 is drawn in connection with the radiation parameter Rd versus the temperature field. Thermal radiation is the discharge of electromagnetic waves from some material. Higher estimates of Rd boosts the temperature. More heat is transferred as Rd is strengthened and this act raises the temperature. The behavior of temperature profile versus varying estimates of the thermophoresis parameter Nt and Brownian motion parameter Nb is illustrated in Figs. 9 and 10 respectively. Thermophoresis is defined as the process with tiny moving particles in mixtures that show distinct responses to the temperature gradient force. Whereas Brownian motion is the random movement of the parti-

cles in a fluid owing to the collision between atoms or molecules. The temperature rises for both parameters. Larger estimates of Nt shift the fluid molecules to the colder zone from the hotter one that eventually boosts the temperature of the fluid. The correlation of the solutal stratification Pw with the concentration profile is displayed in Fig. 11. It is noticed that the concentration of the fluid is on the drop for larger estimates of P . The concentration decreases when the ratio of surface to nanoparticles i.e., the volumetric fraction has waned. Fig. 12 is drawn to reflect the relationship between the motile density stratification parameter Q and the density profile. It is witnessed that the density profile is a dwindling function of Q . The microorganisms' concentration difference at the surface

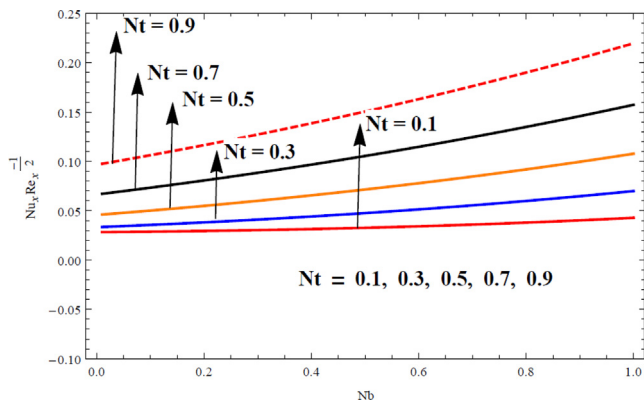


Fig. 16. Effect of $Nu_x Re_x^{-1/2}$ versus varied estimates of Nb and Nt .

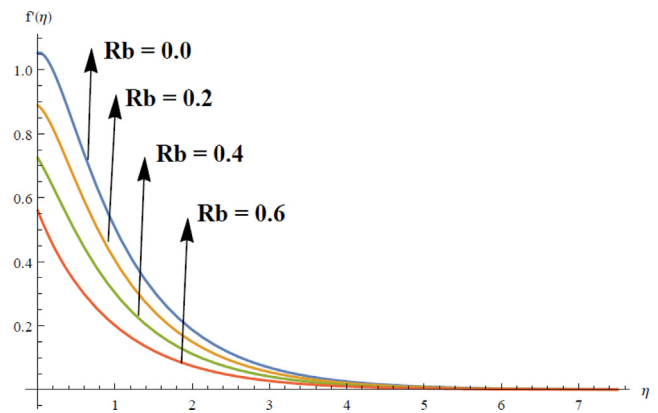


Fig. 19. Response of $f'(\eta)$ versus varied estimates of $Rb = 0.0, 0.2, 0.4, 0.6$.

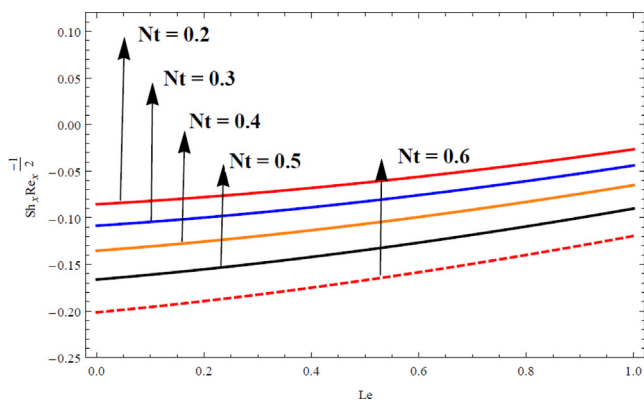


Fig. 17. Effect of $Sh_x Re_x^{-1/2}$ versus varied estimates of Le and Nt .

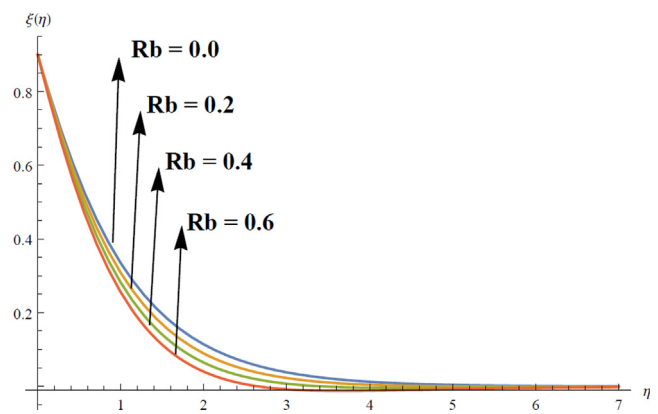


Fig. 20. Response of $\xi(\eta)$ versus varied estimates of $Rb = 0.0, 0.2, 0.4, 0.6$.

Table 2
Comparison of $-f''(0)$ with Andersson (Andersson, 2002) in limiting case while taking all extra parameters as zero.

α	(Andersson, 2002)	Present results
0.0	1.0000	1.000000
0.1	0.8721	0.872092
0.2	0.7764	0.776387
0.5	0.5912	0.591198
1.0	0.4302	0.430182
2.0	0.2840	0.283991
5.0	0.1448	0.144881
10.0	0.0812	0.081211
20.0	0.0438	0.043792
50.0	0.0186	0.018614
100.0	0.0095	0.009521

Table 3
Numerically calculated values of Nusselt number for varied estimates of Rd, Pr, Nb, Nt , and S .

Rd	Pr	Nb	Nt	S	$Nu_x Re_x^{-1/2}$
0.4	1.1	0.2	0.2	0.2	0.000334284
0.6					0.000377515
0.8					0.000416589
	1.1				0.000504542
	1.3				0.000618111
	1.6				0.000819048
		0.1			0.000504147
		0.2			0.000512373
		0.3			0.000583608
			0.2		0.000504542
			0.4		0.000655114
			0.6		0.000703184
				0.2	0.000374193
				0.3	0.000446036
				0.4	0.000504542

Table 4
Numerically calculated values of Sherwood number for varied estimates of Rd, Pr, Nb, Nt , and S .

Le	Pe	Nt	Nb	$Sh_x Re_x^{-1/2}$
0.8	0.1	0.2	0.1	0.00106851
1.0				0.00298939
1.2				0.00303741
	0.1			0.00099662
	0.2			0.00106851
	0.3			0.00114015
		0.2		0.00610151
		0.4		0.00056006
		0.6		0.00052607
			0.1	0.00129005
			0.2	0.00086227
			0.3	0.00018829

and away from the surface is on the decline. That is why density profile in diminished. The response of Motile density field versus Peclet number Pe is displayed in Fig. 13. It is detected that higher estimates of Pe dwindled the Motile density field. As Peclet number is the quotient of heat transfer by fluid motion to the heat transfer through thermal conduction and the microorganism’s diffusivity is an inverse relationship with Peclet number. That is why Motile density field is on the decline for large estimates of Pe . The relationship between bioconvection Lewis number Lb and the motile density is presented in Fig. 14. It is noted that the motile density is the dwindling function of Lb . The diffusivity of the microorganisms is on the decline for larger estimates of Lb that ultimately lowers the motile density of the fluid. This behavior is linked with the feeble diffusivity of microorganisms. Figs. 15–18 portray the impact of

distinct parameters on the Skin friction coefficient, Nusselt, Sherwood, and local density numbers. It is comprehended that for larger estimates of E and Ha , the Skin friction coefficient is augmented. Further, it is understood that Nusselt number is also escalated for growing estimates of Nt and Nb . An opposite trend is witnessed in case of Sherwood number for mounting values of Le and Nt . Also, Nusselt number is increased for higher estimates of Pe and Lb . The effects of bioconvection Rayleigh number Rb versus velocity profile and the Motile density field are displayed in Figs. 19 and 20 respectively. In Fig. 19, it is observed that the velocity of the fluid is on the decline for escalating estimates of Rb . This is due to the increase in the ambient nanoparticle volume fraction and with the buoyancy force owing to bioconvection which hinders the fluid velocity. It is also comprehended that velocity is maximum when $Rb = 0$. Similar behavior for Motile density field is observed for Rb in Fig. 20.

Table 2 is comprised of numerically calculated values of $-f''(0)$ for varied estimates of the slip parameter α in limiting case. The obtained values for $-f''(0)$ are compared with Andersson (Andersson, 2002). From the tabulated estimates, it is observed that an excellent synchronization is obtained between the two comparable results. Tables 3 and 4 are also numerically calculated for Nusselt and Sherwood numbers respectively. It is examined that the numerical calculations are in total harmony with Figs. 16 and 17.

6. Concluding remarks

This exploration discusses the MHD bioconvective Micropolar nanofluid flow with motile microorganisms in a stratified medium. The flow analysis is conducted in the attendance of nonlinear thermal radiation and partial slip condition at the boundary. The Homotopy Analysis Method is used to solve the highly nonlinear system of differential equations. The significant observations of the analysis are:

- Motile density field is on the decline for large estimates of bioconvection Lewis number and Peclet number.
- The fluid velocity is diminished for growing estimates of bioconvection Rayleigh number.
- Velocity is on the decline for higher values of slip and material parameters.
- Hartmann’s number large estimates lower the velocity of the fluid.
- Thermal stratification and radiation boost the temperature of the fluid.
- For thermophoresis and Brownian motion parameters higher estimates, temperature profile rises.
- The velocity is a diminishing function of the suction parameter.

The present exploration may be extended considering some other non-Newtonian fluid. Boundary conditions may be changed to melting heat amalgamated with convective conditions at the surface. The concentration equation may be improved by the addition of chemical reaction effects.

Declaration of Competing Interest

The authors declare that they have no known competing financial interests or personal relationships that could have appeared to influence the work reported in this paper.

Acknowledgments

This work was supported by the Theoretical and Computational Science (TaCS) Center under Computational and Applied Science

for Smart Innovation Research Cluster (CLASSIC), Faculty of Science, KMUTT.

References

- Kuznetsov, A.V., Avramenko, A.A., 2004. Effect of small particles on this stability of bioconvection in a suspension of gyrotactic microorganisms in a layer of finite depth. *Int. Commun. Heat Mass Transfer* 31 (1), 1–10.
- Makinde, O.D., Animasaun, I.L., 2016. Bioconvection in MHD nanofluid flow with nonlinear thermal radiation and quartic autocatalysis chemical reaction past an upper surface of a paraboloid of revolution. *Int. J. Therm. Sci.* 109, 159–171.
- Makinde, O.D., Animasaun, I.L., 2016. Thermophoresis and Brownian motion effects on MHD bioconvection of nanofluid with nonlinear thermal radiation and quartic chemical reaction past an upper horizontal surface of a paraboloid of revolution. *J. Mol. Liq.* 221, 733–743.
- Kuznetsov, A.V., 2010. The onset of nanofluid bioconvection in a suspension containing both nanoparticles and gyrotactic microorganisms. *Int. Commun. Heat Mass Transfer* 37 (10), 1421–1425.
- Nayak, M.K., Prakash, J., Tripathi, D., Pandey, V.S., Shaw, S., Makinde, O.D., 2020. 3D Bioconvective multiple slip flow of chemically reactive Casson nanofluid with gyrotactic micro-organisms. *Heat Trans. –Asian Res.* 49 (1), 135–153.
- Ramzan, M., Mohammad, M., Howari, F., 2019a. Magnetized suspended carbon nanotubes based nanofluid flow with bio-convection and entropy generation past a vertical cone. *Sci. Rep.* 9 (1), 1–15.
- Waqas, H., Khan, S.U., Bhatti, M.M., Imran, M., 2020. Significance of bioconvection in chemical reactive flow of magnetized Carreau-Yasuda nanofluid with thermal radiation and second-order slip. *J. Therm. Anal. Calorim.*, 1–14.
- Khan, M., Salahuddin, T., Malik, M. Y., Alqarni, M. S., & Alqahtani, A. M. (2020). Numerical modeling and analysis of bioconvection on MHD flow due to an upper paraboloid surface of revolution. *Physica A: Statistical Mechanics and its Applications*, 124231.
- Kumar, P.S., Gireesha, B.J., Mahanthesh, B., Chamkha, A.J., 2019. Thermal analysis of nanofluid flow containing gyrotactic microorganisms in bioconvection and second-order slip with convective condition. *J. Therm. Anal. Calorim.* 136 (5), 1947–1957.
- Alshomrani, A.S., Ramzan, M., 2019. Upshot of magnetic dipole on the flow of nanofluid along a stretched cylinder with gyrotactic microorganism in a stratified medium. *Phys. Scr.* 95, (2) 025702.
- Ramzan, M., Chung, J.D., Ullah, N., 2017a. Radiative magnetohydrodynamic nanofluid flow due to gyrotactic microorganisms with chemical reaction and non-linear thermal radiation. *Int. J. Mech. Sci.* 130, 31–40.
- Khan, N.S., Shah, Q., Bhaumik, A., Kumam, P., Thounthong, P., Amiri, I., 2020b. Entropy generation in bioconvection nanofluid flow between two stretchable rotating disks. *Sci. Rep.* 10 (1), 1–26.
- Shahid, A., Zhou, Z., Bhatti, M.M., Tripathi, D., 2018. Magnetohydrodynamics nanofluid flow containing gyrotactic microorganisms propagating over a stretching surface by successive Taylor series linearization method. *Microgravity Sci. Technol.* 30 (4), 445–455.
- Eringen, A.C., 1966. Theory of Micropolar fluids. *J. Mathemat. Mech.*, 1–18
- Turkiymazoglu, M., 2017. Mixed convection flow of magnetohydrodynamic Micropolar fluid due to a porous heated/cooled deformable plate: exact solutions. *Int. J. Heat Mass Transf.* 106, 127–134.
- Ahmad, S., Nadeem, S., Muhammad, N., Khan, M.N., 2020. Cattaneo-Christov heat flux model for stagnation point flow of Micropolar nanofluid toward a nonlinear stretching surface with slip effects. *J. Therm. Anal. Calorim.*, 1–13
- Izadi, M., Sheremet, M.A., Mehryan, S.A.M., Pop, I., Öztop, H.F., Abu-Hamdeh, N., 2020. MHD thermogravitational convection and thermal radiation of a Micropolar nanoliquid in a porous chamber. *Int. Commun. Heat Mass Transfer* 110, 104409.
- Nadeem, S., Malik, M.Y., Abbas, N., 2020. Heat transfer of three-dimensional Micropolar fluid on a Riga plate. *Can. J. Phys.* 98 (1), 32–38.
- Ramzan, M., Farooq, M., Hayat, T., Chung, J.D., 2016. Radiative and Joule heating effects in the MHD flow of a Micropolar fluid with partial slip and convective boundary condition. *J. Mol. Liq.* 221, 394–400.
- Ramzan, M., Ullah, N., Chung, J.D., Lu, D., Farooq, U., 2017b. Buoyancy effects on the radiative magneto Micropolar nanofluid flow with double stratification, activation energy and binary chemical reaction. *Sci. Rep.* 7 (1), 1–15.
- Koriko, O.K., Animasaun, I.L., Omowaye, A.J., Oreyeni, T., 2019. The combined influence of nonlinear thermal radiation and thermal stratification on the dynamics of Micropolar fluid along a vertical surface. *Multidiscipl. Model. Mater. Struct.*
- Ramadevi, B., Kumar, K.A., Sugunamma, V., Reddy, J.R., Sandeep, N., 2020. Magnetohydrodynamic mixed convective flow of Micropolar fluid past a stretching surface using modified Fourier's heat flux model. *J. Therm. Anal. Calorim.* 139 (2), 1379–1393.
- Ramzan, M., Chung, J.D., Ullah, N., 2017c. Partial slip effect in the flow of MHD Micropolar nanofluid flow due to a rotating disk—A numerical approach. *Results Phys.* 7, 3557–3566.
- Gireesha, B.J., Mahanthesh, B., Thammanna, G.T., Sampathkumar, P.B., 2018. Hall effects on dusty nanofluid two-phase transient flow past a stretching sheet using KVL model. *J. Mol. Liq.* 256, 139–147.
- Mahanthesh, B., Shashikumar, N.S., Gireesha, B.J., Animasaun, I.L., 2019. Effectiveness of Hall current and exponential heat source on unsteady heat transport of dusty TiO₂-EO nanoliquid with nonlinear radiative heat. *J. Comput. Des. Eng.* 6 (4), 551–561.
- Sheikholeslami, M., 2019. New computational approach for exergy and entropy analysis of nanofluid under the impact of Lorentz force through a porous media. *Comput. Methods Appl. Mech. Eng.* 344, 319–333.
- Mahanthesh, B., Shehzad, S.A., Ambreen, T., Khan, S.U., 2020. Significance of Joule heating and viscous heating on heat transport of MoS₂-Ag hybrid nanofluid past an isothermal wedge. *J. Therm. Anal. Calorim.*, 1–9
- Lu, D., Ramzan, M., Ahmad, S., Chung, J.D., Farooq, U., 2018a. A numerical treatment of MHD radiative flow of Micropolar nanofluid with homogeneous-heterogeneous reactions past a nonlinear stretched surface. *Sci. Rep.* 8 (1), 1–17.
- Wakif, A., Animasaun, I. L., PV, S. N., & Sarojamma, G. (2019). Meta-analysis on thermo-migration of tiny/nano-sized particles in the motion of various fluids. *Chinese Journal of Physics*, doi.org/10.1016/j.cjph.2019.12.002
- Animasaun, I.L., Ibraheem, R.O., Mahanthesh, B., Babatunde, H.A., 2019. A meta-analysis on the effects of haphazard motion of tiny/nano-sized particles on the dynamics and other physical properties of some fluids. *Chin. J. Phys.* 60, 676–687.
- Gireesha, B.J., Mahanthesh, B., Makinde, O.D., Muhammad, T., 2018. Effects of Hall current on transient flow of dusty fluid with nonlinear radiation past a convectively heated stretching plate. *Defect Diffus. Forum* 387, 352–363.
- Hajizadeh, M.R., Selimefendigil, F., Muhammad, T., Ramzan, M., Babazadeh, H., Li, Z., 2020. Solidification of PCM with nano powders inside a heat exchanger. *J. Mol. Liq.* 306, 112892.
- Kumar, P.S., Mahanthesh, B., Gireesha, B.J., Shehzad, S.A., 2018. Quadratic convective flow of radiated nano-Jeffrey liquid subject to multiple convective conditions and Cattaneo-Christov double diffusion. *Appl. Math. Mech.* 39 (9), 1311–1326.
- Tlili, I., Naseer, S., Ramzan, M., Kadry, S., Nam, Y., 2020. Effects of chemical species and nonlinear thermal radiation with 3D Maxwell nanofluid flow with double stratification—An analytical solution. *Entropy* 22 (4), 453.
- Mahanthesh, B., Lorenzini, G., Oudina, F.M., Animasaun, I.L., 2019. Significance of exponential space-and thermal-dependent heat source effects on nanofluid flow due to radially elongated disk with Coriolis and Lorentz forces. *J. Therm. Anal. Calorim.*, 1–8
- Alebraheem, J., Ramzan, M., 2019. Flow of nanofluid with Cattaneo-Christov heat flux model. *Applied Nanoscience*, 1–11.
- Turkiymazoglu, M., 2019. Free and circular jets cooled by single phase nanofluids. *Eur. J. Mech. B/Fluids* 76, 1–6.
- Turkiymazoglu, M., 2018. Buongiorno model in a nanofluid filled asymmetric channel fulfilling zero net particle flux at the walls. *Int. J. Heat Mass Transf.* 126, 974–979.
- Ahmad, R., Mustafa, M., Turkiymazoglu, M., 2017. Buoyancy effects on nanofluid flow past a convectively heated vertical Riga-plate: a numerical study. *Int. J. Heat Mass Transf.* 111, 827–835.
- Nayak, M.K., Prakash, J., Tripathi, D., Pandey, V.S., 2019. 3D radiative convective flow of ZnO-SAE50nano-lubricant in presence of varying magnetic field and heterogeneous reactions. *Propul. Power Res.* 8 (4), 339–350.
- Akbar, N.S., Tripathi, D., Khan, Z.H., 2018. Numerical investigation of Cattaneo-Christov heat flux in CNT suspended nanofluid flow over a stretching porous surface with suction and injection. *Discrete & Continuous Dynam. Syst. -S* 11 (4), 583–594.
- Nayak, M.K., Akbar, N.S., Tripathi, D., Pandey, V.S., 2017. Three dimensional MHD flow of nanofluid over an exponential porous stretching sheet with convective boundary conditions. *Ther. Sci. Eng. Prog.* 3, 133–140.
- Nayak, M.K., Akbar, N.S., Tripathi, D., Khan, Z.H., Pandey, V.S., 2017. MHD 3D free convective flow of nanofluid over an exponentially stretching sheet with chemical reaction. *Adv. Powder Technol.* 28 (9), 2159–2166.
- Turkiymazoglu, M., 2019. Fully developed slip flow in a concentric annuli via single and dual phase nanofluids models. *Comput. Methods Programs Biomed.* 179, 104997.
- Sheikholeslami, M., Sheremet, M.A., Shafee, A., Li, Z., 2019. CVFEM approach for EHD flow of nanofluid through porous medium within a wavy chamber under the impacts of radiation and moving walls. *J. Therm. Anal. Calorim.* 138 (1), 573–581.
- Ramzan, M., Mohammad, M., Howari, F., Chung, J.D., 2019b. Entropy analysis of carbon nanotubes based nanofluid flow past a vertical cone with thermal radiation. *Entropy* 21 (7), 642.
- Turkiymazoglu, M., 2019. MHD natural convection in saturated porous media with heat generation/absorption and thermal radiation: closed-form solutions. *Arch. Mech.* 71 (1), 49–64.
- Bilal, M., Ramzan, M., 2019. Hall current effect on unsteady rotational flow of carbon nanotubes with dust particles and nonlinear thermal radiation in Darcy-Forchheimer porous media. *J. Therm. Anal. Calorim.* 138 (5), 3127–3137.
- Turkiymazoglu, M., 2016. Natural convective flow of nanofluids past a radiative and impulsive vertical plate. *J. Aerosp. Eng.* 29 (6), 04016049.
- Ramzan, M., Bilal, M., Chung, J.D., 2017d. Effects of thermal and solutal stratification on Jeffrey magneto-nanofluid along an inclined stretching cylinder with thermal radiation and heat generation/absorption. *Int. J. Mech. Sci.* 131, 317–324.
- Li, Z., Sheikholeslami, M., Shafee, A., Ramzan, M., Kandasamy, R., Al-Mdallal, Q.M., 2019. Influence of adding nanoparticles on solidification in a heat storage system considering radiation effect. *J. Mol. Liq.* 273, 589–605.
- Sheikholeslami, M., Shafee, A., Ramzan, M., Li, Z., 2018. Investigation of Lorentz forces and radiation impacts on nanofluid treatment in a porous semi annulus via Darcy law. *J. Mol. Liq.* 272, 8–14.
- Suleman, M., Ramzan, M., Zulfikar, M., Bilal, M., Shafee, A., Chung, J.D., Farooq, U., 2018. Entropy analysis of 3D non-newtonian MHD nanofluid flow with

- nonlinear thermal radiation past over exponential stretched surface. *Entropy* 20 (12), 930.
- Lu, D., Ramzan, M., Ahmad, S., Shafee, A., Suleman, M., 2018b. Impact of nonlinear thermal radiation and entropy optimization coatings with hybrid nanoliquid flow past a curved stretched surface. *Coatings* 8 (12), 430.
- Waqas, M., Dogonchi, A.S., Shehzad, S.A., Khan, M.I., Hayat, T., Alsaedi, A., 2020. Nonlinear convection and joule heating impacts in magneto-thixotropic nanofluid stratified flow by convectively heated variable thicked surface. *J. Mol. Liq.* 300, 111945.
- Ramzan, M., Shaheen, N., Kadry, S., Ratha, Y., Nam, Y., 2020. Thermally stratified Darcy Forchheimer flow on a moving thin needle with homogeneous heterogeneous reactions and non-uniform heat source/sink. *Appl. Sci.* 10 (2), 432.
- Ahmad, S., Nadeem, S., Muhammad, N., & Issakhov, A. (2020). Radiative SWCNT and MWCNT nanofluid flow of Falkner–Skan problem with double stratification. *Physica A: Statistical Mechanics and its Applications*, 124054.
- Daniel, Y.S., Aziz, Z.A., Ismail, Z., Bahar, A., 2020. Unsteady EMHD dual stratified flow of nanofluid with slips impacts. *Alexandria Eng. J.* 59 (1), 177–189.
- Ramzan, M., Gul, H., Kadry, S., 2019c. Onset of Cattaneo-Christov heat flux and thermal stratification in ethylene-glycol based nanofluid flow containing carbon nanotubes in a rotating frame. *IEEE Access* 7, 146190–146197.
- Naz, R., Noor, M., Shah, Z., Sohail, M., Kumam, P., Thounthong, P., 2020. Entropy generation optimization in MHD pseudoplastic fluid comprising motile microorganisms with stratification effect. *Alexandria Eng. J.* 59 (1), 485–496.
- Rosseland, S. (2013). *Astrofysik: Auf Atomtheoretischer Grundlage* (Vol. 11). Springer-Verlag.
- Khan, N.S., Gul, T., Khan, M.A., Bonyah, E., Islam, S., 2017. Mixed convection in gravity-driven thin film non-Newtonian nanofluids flow with gyrotactic microorganisms. *Results Phys.* 7, 4033–4049.
- Andersson, H.I., 2002. Slip flow past a stretching surface. *Acta Mech.* 158 (1–2), 121–125.